Microscopy Study of the Growth Process and Structural Features of Closely Packed Silica Nanowires

Shuhui Sun,*,† Guowen Meng,*,†,‡ Mingang Zhang,†,§ Yufeng Hao,† Xueru Zhang,† and Lide Zhang†

Institute of Solid State Physics, Chinese Academy of Sciences, Hefei 230031, P. R. China, Department of Materials Science and Engineering, Rensselaer Polytechnic Institute, 1108th Street, Troy, New York 12180, and Department of Materials Science and Engineering, Taiyuan Heavy Machinery Institute, Taiyuan 030024, P. R. China

Received: June 21, 2003

This article describes for the first time the direct observation of the nucleation and growth process of closely packed silica nanowires via a vapor−liquid−solid (VLS) mechanism by using tin (Sn) as a catalyst. Initially, Sn particles formed alloy liquids, followed by the nucleation of short silica nanowires, and closely packed silica nanowires finally formed. Interestingly, our results indicated that Sn has different catalytic behavior for nanowire growth than commonly used metal catalysts such as Au and Fe. The structural features associated with different growth stages were monitored by SEM, TEM, EDX, and XPS analysis. A possible mechanism for the formation of closely packed silica nanowires is proposed.

1. Introduction

In recent years, 1D nanomaterials have attracted much attention because of their fundamental importance to the study of size- and dimensionality-dependent chemical and physical properties and their great potential for nanoscale electronics and opotoelectronics.[1,2] Silicon oxide (SiO_2), as an important candidate for photoluminescence (PL) materials, has been actively studied for a long time. The PL band of bulk SiO_2 or SiO_2 films has a peak around 1.9−4.3 eV.[3,4] SiO_2 nanowires have been prepared by several methods.[5−8] Yu et al.[5] have synthesized SiO_2 nanowires using an excimer laser ablation method and have investigated their intense blue-light emission. Other methods such as sol−gel,[6] carbothermal reduction,[7] and chemical vapor deposition (CVD)[8] have also been applied to the synthesis of SiO_2 nanowires.

It is of interest that silicon oxide may form some novel morphologies such as silica "nanoflowers",[9,10] radial patterns of carbonated silica fibers,[11,12] silica nanowire "bundles" and "nanobrush" arrays and silica nanotubes,[13] and treelike and tadpolelike SiO_x nanostructures.[14] Very recently, Liu et al.[15] have synthesized ultralong and highly oriented silicon oxide nanowires via Ga as a catalyst; Pan and co-workers push the conventional VLS mechanism to a new range by using molten gallium as a catalyst to grow highly aligned silica nanowires.[16] Recently, we generated large quantities of closely packed silica nanowire bunches by using tin (Sn) powder as a catalyst and silicon wafers as a source material via the extended VLS mechanism proposed by Pan et al.[16] The growth mechanism could also give an important clue to the improvement in the quality of the grown nanowires. Direct evidence for the extended VLS mechanism, however, is still lacking except for the fact that nanowires have alloy droplets on their tips. Hence, more detailed and systematic experimental investigations are required.

Herein, we have systematically investigated the growth process of closely packed silica nanowires catalyzed by Sn. On the basis of our results, three well-defined stages have been clearly identified during the process: the growth of Sn particles and metal alloying, the nucleation of short silica nanowires, and the growth of closely packed silica nanowires.

2. Experimental Section

The synthesis of silica nanostructures was carried out in a high-temperature tube furnace. Briefly, an alumina tube was placed horizontally inside the tube furnace. An alumina boat loaded with pure Sn powder (99.9 wt %, 0.1 g) was placed in the center of the alumina tube, and several pretreated Si wafers were placed one by one on a long alumina plate, which was placed next to the alumina boat at the downstream end of the tube. Before heating, the tube was evacuated by a mechanical rotary pump to a base pressure of 5×10^{-2} Torr. High-purity argon (99.99%, $H_2O \leq 20$ ppm, $O_2 \leq 20$ ppm) was then used to clean away the impurity gas absorbed in the Si wafers, alumina boat and plate, and tube wall. High-purity argon was kept flowing through the tube during the experiment at a rate of 100 sccm (standard cubic centimeters per minute), and the flow pressure in the alumina tube was kept at about 1 atm. Then, the furnace was heated to 980 °C quickly. A series of experiments were performed with different heating-time durations of 5, 15, 30, 45, 60, and 120 min, and other parameters were kept the same.

After the experiments, the as-synthesized products were characterized by scanning electron microscopy (SEM, JEOL JSM-6300) and transmission electron microscopy (TEM, JEM-200CX at 200 kV). The chemical compositions were determined by X-ray photoemission spectra (XPS, VGESCALAB MKII) and an energy-dispersive X-ray spectroscope (EDS) attached to the SEM instrument. XPS data were collected in the constant

* To whom correspondence should be addressed. E-mail: shsuncn@hotmail.com (Shuhui Sun) and gwmeng@issp.ac.cn (Guowen Meng). Fax: +86-551-5591434.

† Chinese Academy of Sciences.

‡ Rensselaer Polytechnic Institute.

§ Taiyuan Heavy Machinery Institute.

10.1021/jp035763y CCC: $25.00
Published on Web 11/01/2003

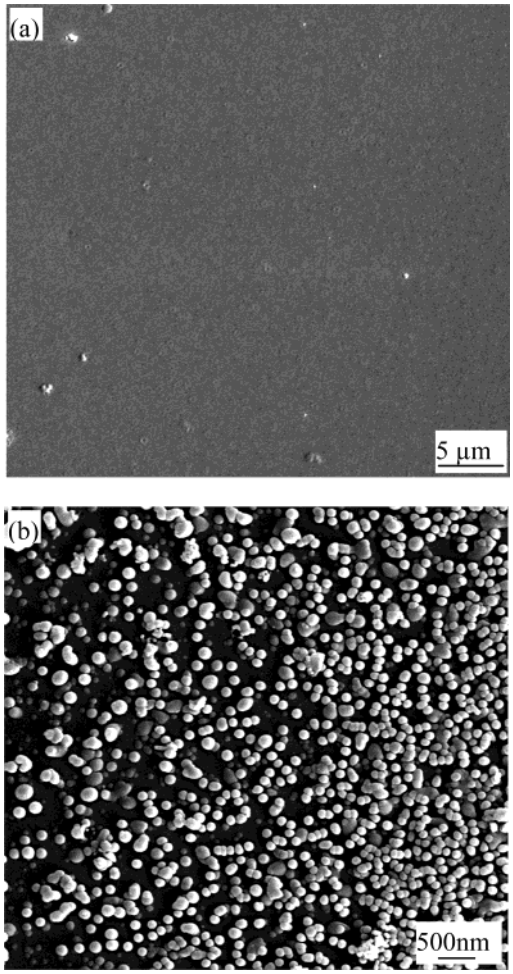

Figure 1. SEM images of a Si wafer. (a) After 5 min of heating. (b) After 15 min of heating, the Si wafer is covered with nanosized uniform particles.

analyzer energy (CAE) mode at 20 eV. Mg Kα ($h\nu$ = 1253.6 eV) radiation was employed as the excitation source with an anode voltage of 12 kV and an emission current of 20 mA. For SEM observations, the product was presputtered with a conducting layer of noble Pt metal and then together with the Si wafer was directly transferred into the SEM chamber. Specimens for TEM investigations were briefly ultrasonicated in ethanol, and then a drop of suspension was placed on a holey carbon copper grid.

3. Results and Discussion

Figures 1−4 show a sequence of SEM images during the growth process of closely packed silica nanowires. These observations of the nanowires' growth directly mirror the proposed VLS mechanism in Figure 6. In general, three stages could be clearly identified.

3.1. Initial Stage (≤15 min): Growth of Sn Nanoparticles and Alloying Process (Figure 1a and b). Figure 1a shows that after heating at 980 °C for 5 min, there has been no significant change in the Si wafer; however, Sn nanoclusters, generated from the thermal evaporation of Sn powder, have started to deposit onto the surface of silicon wafers to grow into small liquid Sn droplets. With increasing amounts of Si vapor generated from the thermal evaporation of Si wafers followed by condensation and dissolution, Si and Sn then form alloy droplets,[17] which can be adjudged from EDS analysis. The diameters of alloy droplets increase with the reaction time through continuously accepting the incoming Sn and Si species from the vapor. After 15 min, the diameters of the alloy droplets are in the range of 75 to 150 nm (as shown in Figure 1b).

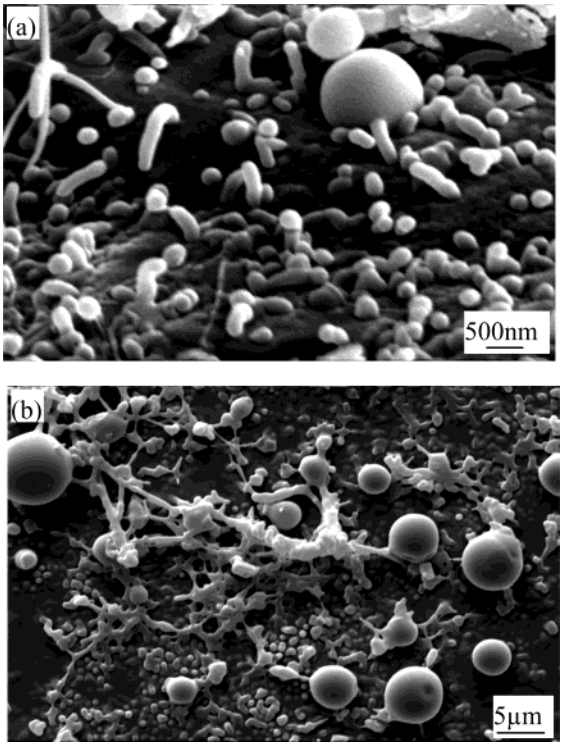

Figure 2. (a) SEM image after 30 min of heating; nanowires nucleate and start to grow out from the balls. (b) SEM image after 45 min of heating; nanowires continue to grow, and the balls grow larger.

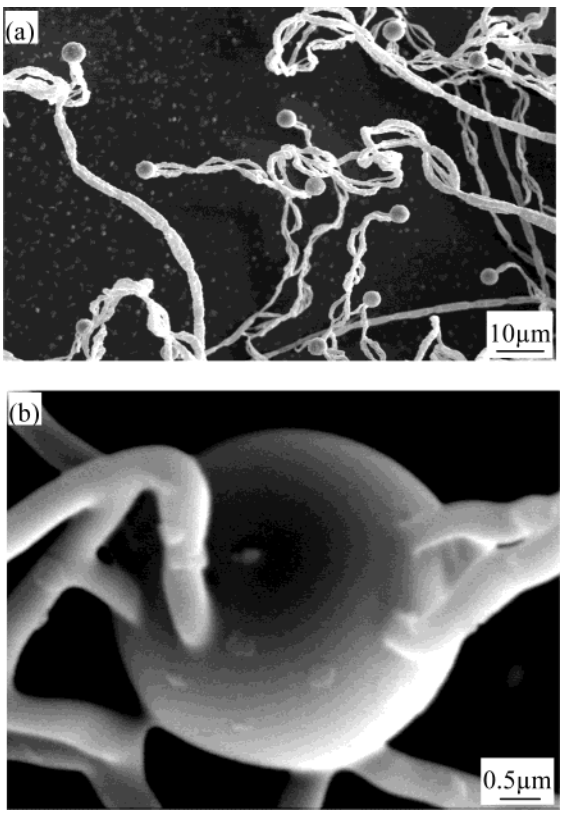

Figure 3. SEM images taken after 60 min of heating. (a) Low-magnification image reveals the cherrylike structure of the products. (b) High-magnification view shows that several nanowires grow out from the lower surface of the spheroid and that several nanoparticles appear on the surface of the spheroid, indicating the initiating nucleation.

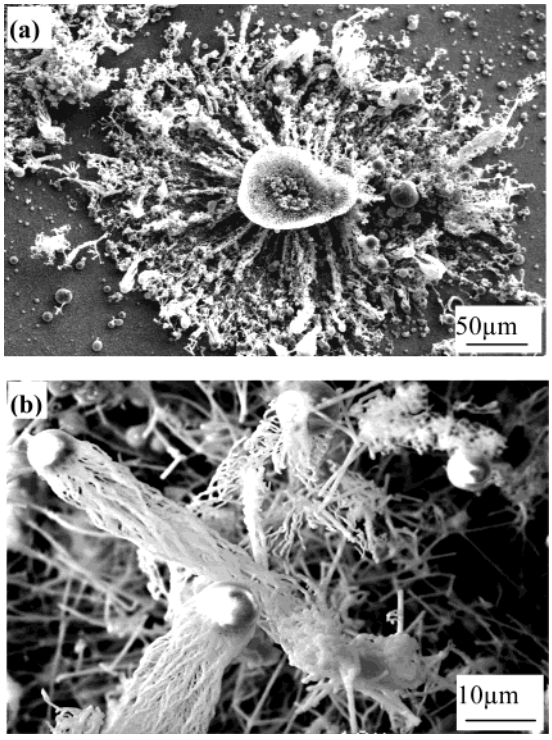

Figure 4. SEM images after 120 min of heating. (a) Low-magnification image shows a large quantity of the closely packed oriented nanowires. (b) High-magnification of the novel structures of oriented silica nanowires.

3.2. Second Stage (15−45 min): Nucleation (Figure 2a and b). As the heating process continues, short SiO_2 nanowires will form. As shown in Figure 2a (after 30 min of heating), the nucleation seems to initiate from the lower surface of the alloy particles (i.e., at the tip of most of the short nanowires, 50−100 nm in diameter); round balls with diameters that are 1.5 to 2 times that of the connected nanowire are observed. This corresponds to the morphology of VLS-grown nanowires, suggesting that the growth of the nanowires is likely governed by the VLS mechanism.[18] Also, a few of the nanowires are capped with balls with a diameter that is 10 times larger than the diameter of the nanowires. Figure 2b is a top SEM image after 45 min of heating; it can be seen that the balls grow larger, with diameters in the range of 1 to 6 μm.

3.3. Final Stage (45−120 min): Growth of Nanowires (Figure 3a and b, Figure 4a and b). Extending the heating time elongated the nanowires and enlarged the balls connected with the nanowires. Figure 3 shows the SEM images at a heating time of 60 min. A typical low SEM image (Figure 3a) shows an intermediate stage in the nanowires' growth. In fact, each ball attaches to many nanowires that grow out perpendicularly from the surface of the ball's lower hemisphere. That means that each ball can simultaneously catalyze the growth of many nanowires; this phenomenon is similar to that observed by Pan et al.[16] in their Ga-catalyzed SiO_2 nanofibers. A closer inspection (Figure 3b) reveals that some nanowires grow out from the surface of the ball, with many nanoparticles appearing on the surface of the ball, and splitting growth can also be observed. Finally, well-developed oriented closely packed silica nanowires are produced after 120 min of heating (Figure 4a). A representative high-magnification SEM image (Figure 4b) reveals the novel structures of the product. Each novel structure terminates at its top end in a large spherical ball with a diameter comparable to that of the connected tail (Figure 1b). The tail part of the novel structure is composed of large quantities of closely packed

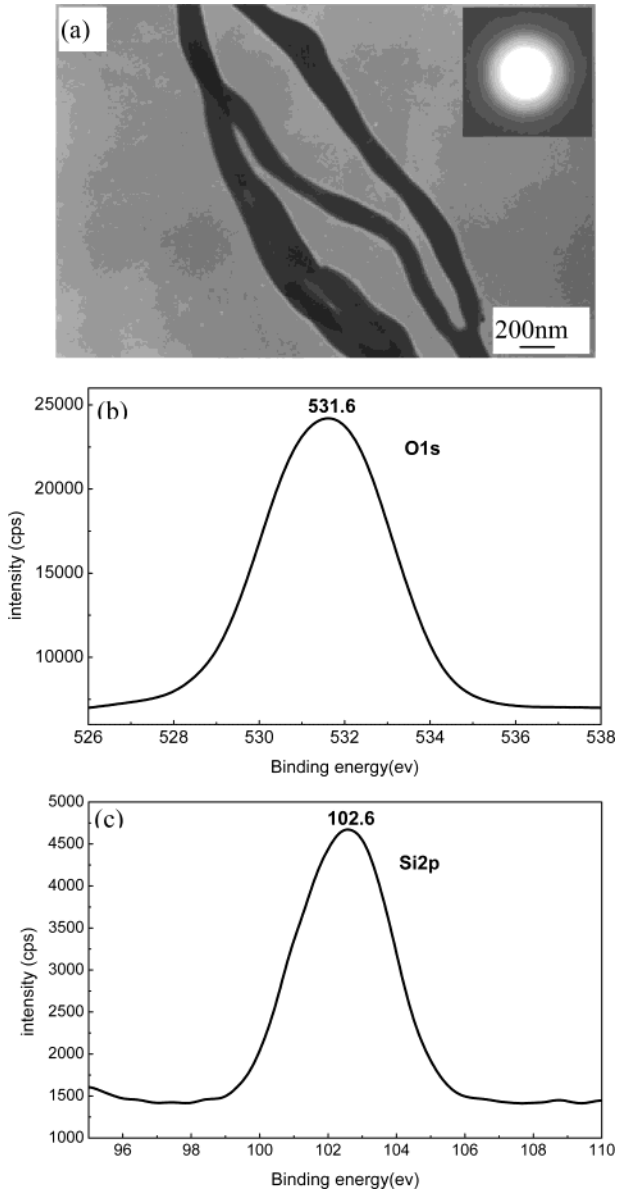

Figure 5. (a) TEM image of the as-synthesized nanowires, and the highly dispersed SAED ring pattern (inset) showing that the nanowires are amorphous. XPS spectra of the silica nanowires. (b) O 1s binding-energy spectrum. (c) Si 2p binding-energy spectrum.

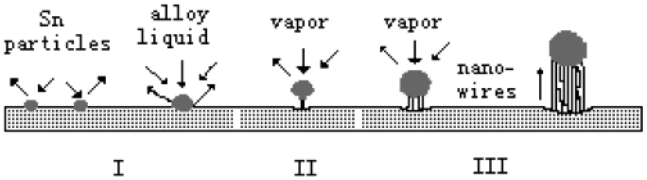

Figure 6. Proposed model for the growth of oriented silica nanowires including three stages of (I) the growth of Sn nanoparticles and the alloying process, (II) nucleation, and (III) the growth of nanowires.

oriented nanowires with diameters of 100−200 nm and lengths of 50−100 μm. EDS analysis taken from the ball reveals the presence of Sn, Si, and O. However, quantitative EDS analyses of the nanowires show that the nanowires have a composition close to SiO_2. DES analysis further supports the VLS growth process of silica nanowires.

The morphology and structure of the nanowires have been characterized in further detail using TEM. The nanowires (Figure 5a) have smooth surfaces with diameters of about 100−200 nm, and the split growth of SiO_2 nanowires occurs, in agreement

with SEM observations. A highly dispersed selected-area electron diffraction pattern (inset in Figure 5a) taken from many nanowires shows that the SiO_2 nanowires are amorphous. Further evidence for the formation of silica nanowires can be obtained through XPS. The two strong peaks at 531.6 and 102.6 eV as shown in Figure 5b and c correspond to the binding energy of O (1s) and Si (2p) to silica, respectively.

4. Discussion

The experimental results described in section 3 show the different growth stages of oriented silica nanowires by heating Si wafers to 980 °C for different times via Sn powder as a catalyst under flowing Ar gas (100 sccm). Our systematic experiments at varied heating times (5−120 min) show that the product development was strongly related to the heating duration. The alloying, nucleation, and growth of product can be observed with the heating process. The experimental results show that low-melting-point Sn can serve as an effective catalyst for the growth of amorphous silica nanowires via the VLS mechanism. However, our results indicated that Sn shows different catalytic behavior for nanowire growth, which is similar to that observed in Ga-catalyst growth of aligned silica nanowires from commonly used metal catalysts such as Au and Fe. On the basis of the experimental results described above and the VLS mechanism, a growth model (depicted in Figure 6) is proposed for the novel structures grown on Si wafers. Si wafers were first dissolved in molten Sn, which was transported from the thermal evaporation of Sn powder at elevated temperature. The solubility of Si in Sn at 950 °C is ∼4 atom %.[17] The Si in the Sn−Si alloy evaporates into gas species to create a dense vapor of silicon species around the silicon wafers region. Meanwhile, the liquid alloy droplets could also absorb Si from the vapor. Then the dissolved Si was oxidized by oxygen from the low content of H_2O (∼20 ppm) and O_2 (∼20 ppm) in the carrier gas of Ar. Because silicon oxide is not soluble in tin, it had to precipitate out of the alloy liquid in a certain form, for example, silicon oxide nanoparticles. This is the driving force for nanowire growth. If many nanoparticles precipitate out of the same one-alloy liquid simultaneously or subsequently, it may lead to many nanowires growing out of one ball. Perhaps this is the reason that one low-melting-point metal ball can simultaneously catalyze the growth of many SiO_2 nanowires.

Although only the heating duration was discussed in this paper, other experimental parameters such as the heating temperature, gas flow rate, and pressure in the chamber also influence nanostructure development. The growth of these novel silica nanowire structures catalyzed via Sn is a rather complicated process, and many issues remain open. More work is underway to understand better the growth mechanism and to prepare nanowires with different diameters and/or different materials.

5. Conclusions

Oriented, closely packed silica nanowires have been grown by heating Si wafers via Sn powder as a catalyst. Direct SEM observation of the growth process of silica nanowires reveals that the growth involves three stages: the growth of Sn nanoparticles and the alloying process, the nucleation of silica nanowires, and the growth of silica nanowires. The process appears to involve an extended VLS mechanism, which is different from the conventional VLS mechanism. Many silicon oxide nanoparticles precipitate out of the same one-alloy liquid simultaneously or subsequently, possibly leading to many nanowires growing out of the same ball.

Acknowledgment. We thank Professor Yongqiang Mao and Zhaoqin Chu for their technical assistance. This work was supported by the Ministry of Science and Technology of China (grant no. G1999064501) and the National Natural Science Foundation of China (grant no. 19974055).

References and Notes

(1) Han, J.; Fan, S.; Li, Q.; Hu, Y. *Science* **1997**, *277*, 1287.
(2) Ruecks, T.; Kim, K.; Joselevich, E.; Tseng, G. Y.; Cheung, C.; Lieber, C. M. *Science* **2000**, *289*, 94.
(3) Liao, L. S.; Bao, X. M.; Zheng, X. Q.; Li, N. S.; Min, N. B. *Appl. Phys. Lett.* **1996**, *68*, 850.
(4) Nishikawa, H.; Shiroyama, T.; Nakamura, R.; Ohiki, Y.; Nagasawa, K.; Hama, Y. *Phys. Rev. B* **1992**, *45*, 586.
(5) Yu, D. P.; Hang, Q. L.; Ding, Y.; Zhang, H. Z.; Bai, Z. G.; Wang, J. J.; Zou, Y. H. *Appl. Phys. Lett.* **1998**, *73*, 3076.
(6) Zhang, M.; Bando, Y.; Wada, L.; Kurashima, K. *J. Mater. Sci. Lett.* **1999**, *18*, 1911.
(7) Wu, X. C.; Song, W. H.; Wang, K. Y.; Hu, T.; Zhao, B.; Sun, Y. P.; Du, J. J. *Chem. Phys. Lett.* **2001**, *53*, 366.
(8) Liu, Z. Q.; Xie, S. S.; Sun, L. F.; Tang, D. S.; Zhou, W. Y.; Wang, C. Y.; Liu, W.; Li, Y. B.; Zou, X. P.; Wang, G. *J. Mater. Res.* **2001**, *16*, 683.
(9) Zhu, Y. Q.; Hsu, W. H.; Terrones, M.; Grobert, N.; Terrones, M.; Hare, J. P.; Kroto, H. W.; Walton, D. R. M. *J. Mater. Chem.* **1998**, *8*, 1859.
(10) Zhu, Y. Q.; Hu, W. B.; Hsu, W. H.; Terrones, M.; Grobert, N.; Karali, T.; Terrones, M.; Hare, J. P.; Townsend, P. D.; Kroto, H. W.; Walton, D. R. M. *Adv. Mater.* **1999**, *11*, 844.
(11) Zhang, Z. J.; Ramanath, G.; Ajiayan, P. M.; Goldberg, D.; Bande, Y. *Adv. Mater.* **2001**, *13*, 197.
(12) Zhang, Z. J.; Ajiayan, P. M.; Ramanath, G. *Appl. Phys. Lett.* **2001**, *78*, 3794.
(13) Wang, Z. L.; Gao, R. P.; Gole, J. L.; Stout, J. D. *Adv. Mater.* **2000**, *12*, 1938.
(14) Chen, Y. J.; Li, J. B.; Dai, J. H. *Chem. Phys. Lett.* **2001**, *344*, 450.
(15) Zheng, B.; Wu, Y. Y.; Yang, P. D.; Liu, J. *Adv. Mater.* **2002**, *14*, 122.
(16) Pan, Z. W.; Dai, Z. R.; Ma, C.; Wang, Z. L. *J. Am. Chem. Soc.* **2002**, *124*, 1817.
(17) Massalski, T. B.; Okamoto, H.; Subramanian, P. R.; Kacprozak, L. *Binary Alloy Phase Diagrams*, 2nd ed.; ASM Int.: Materials Park, OH, 1992.
(18) Wagner, R. S.; Ellis, W. C. *Appl. Phys. Lett.* **1964**, *4*, 89.